Title
INFLUENCE OF IMPURITY SEGREGATION ON TEMPER EMBRITTLEMENT AND ON SLOW FATIGUE CRACK GROWTH AND THRESHOLD BEHAVIOR IN 300-M HIGH STRENGTH STEEL

Author
Ritchie, Robert O.

Publication Date
1976-10-01

Submitted to Metallurgical Transactions A

LBL-5498
Preprint

INFLUENCE OF IMPURITY SEGREGATION ON TEMPER EMBRITTLEMENT AND ON SLOW FATIGUE CRACK GROWTH AND THRESHOLD BEHAVIOR IN 300-M HIGH STRENGTH STEEL

Robert O. Ritchie

October 1976

Prepared for the U. S. Energy Research and
Development Administration under Contract W-7405-ENG-48

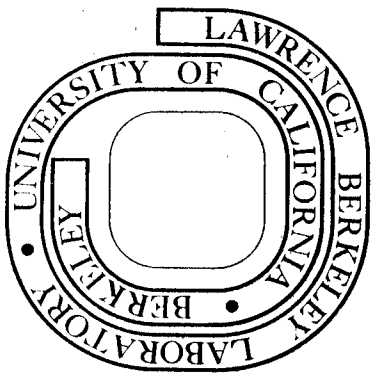

DISCLAIMER

INFLUENCE OF IMPURITY SEGREGATION ON TEMPER EMBRITTLEMENT AND ON SLOW FATIGUE CRACK GROWTH AND THRESHOLD BEHAVIOR IN 300-M HIGH STRENGTH STEEL

Robert O. Ritchie*

Materials and Molecular Research Division, Lawrence Berkeley Laboratory
and Department of Materials Science and Engineering,
University of California, Berkeley, California 94720

ABSTRACT

Interactions between hydrogen embrittlement and temper embrittlement have been examined in a study of fracture and low growth rate (near-threshold) fatigue crack propagation in 300-M high strength steel, tested in humid air. The steel was investigated in an unembrittled condition (oil quenched after tempering at 650°C) and temper embrittled condition (step-cooled after tempering at 650°C). Step-cooling resulted in a severe loss of toughness (approximately 50 pct reduction), without loss in strength, concurrent with a change in fracture mode from microvoid coalescence to intergranular. Using Auger spectroscopy analysis, the embrittlement was attributed to the co-segregation of alloying elements (Ni and Mn) and impurity elements (P and Si) to prior austenite grain boundaries. Prior temper embrittlement gave rise to a substantial reduction in resistance to fatigue crack propagation, particularly at lower stress intensities approaching the threshold for crack growth (ΔK_o). At intermediate growth rates (10^{-5} - 10^{-3} mm/cycle), propagation rates in

---

*Now at Department of Mechanical Engineering, Massachusetts Institute of Technology, Cambridge, MA 02139.

both unembrittled and embrittled material were largely similar, and only weakly dependent on the load ratio, consistent with the striation mechanism of growth observed. At near-threshold growth rates ($< 10^{-5} - 10^{-6}$ mm/cycle), embrittled material exhibited significantly higher growth rates, 30 pct reduction in threshold ΔK_o values and intergranular facets on fatigue fracture surfaces. Near-threshold propagation rates (and ΔK_o values) were also found to be strongly dependent on the load ratio. The results are discussed in terms of the combined influence of segregated impurity atoms (temper embrittlement) and hydrogen atoms, evolved from crack tip surface reactions with water vapor in the moist air environment (hydrogen embrittlement). The significance of crack closure concepts on this model is briefly described.

INTRODUCTION

It is well known that the toughness of Ni-Cr containing alloy steel can be severely reduced by the segregation and build-up of residual impurity elements (eg. S, P, Sb, Sn, etc.) in grain boundaries when the steel is tempered in, or slowly cooled through, the range ~300-550°C.[1] The result of this embrittlement is generally brittle fracture along prior austenite grain boundaries, although intergranular fracture along ferritic boundaries can also occur.[2,3] The loss in toughness can result primarily from two types of thermal treatments: i) tempering of as-quenched alloy steels in the range 300-450°C ("tempered martensite" or "500°F" or "350°C" or "one-step temper" embrittlement),[4-6] and ii) holding or slow cooling alloy steels, previously tempered above 650°C, in the temperature range 550-350°C (temper embrittlement).[1-6] This "micro-pollution" of interfaces with impurities, resulting from such treatments, can also degrade other fracture properties in alloy steels. Resistance to fatigue crack propagation at high growth rates ($> 10^{-4}$ mm/cycle) is often significantly reduced by prior temper embrittlement, involving the occurrence of brittle intergranular cracking during fatigue striation growth.[7] Creep rupture ductility has similarly been observed to be severely impaired by the presence of impurities.[8] The deterioration in fracture properties can be even more pronounced when environmentally-induced fractures, particularly those involving hydrogen, are considered. In commercial HY130 steel, for example, the susceptibilities to stress corrosion cracking in sulfuric acid,[9] and hydrogen-assisted cracking in gaseous hydrogen,[10] are

significantly increased when the material is heat-treated to induce temper embrittlement. Similar effects have been seen with embrittled 4340 steel tested in hydrogen[10] and hydrogen sulfide.[11] Clearly a strong interaction exists between hydrogen- and impurity-induced embrittlement. Both forms of embrittlement generally lower the grain boundary strength, increasing the tendency for intergranular fracture around prior austenite grains. The dependence on matrix hardness is similar in both cases, and, furthermore, the 'tramp' elements that lead to temper embrittlement through segregation to grain boundaries also assist hydrogen-induced cracking by acting as re-combination poisons for atomic hydrogen.[11]

The present study was instigated to examine the possibility of an effect of prior temper embrittlement on fatigue crack propagation in humid air at extremely low growth rates ($< 10^{-5} - 10^{-6}$ mm/cycle) approaching the threshold stress intensity (ΔK_o), below which fatigue crack growth cannot be detected. A quenched and tempered high strength steel (300-M) was chosen for the investigation, since hydrogen embrittlement has been generally regarded as the primary mechanism of environmental attack during fatigue crack growth in such steels in the presence of moisture.[12]

EXPERIMENTAL PROCEDURES

The 300-M steel used for the study was of aircraft-quality (vacuum-arc remelted), received as hot-rolled bar in the fully annealed condition. The composition in wt. pct. is shown below:

C	Mn	Cr	Ni	Mo	Si	S	P	V
0.42	0.76	0.76	1.76	0.41	1.59	0.002	0.007	0.10

The material was austenitized for 1 hr at 870°C and quenched into agitated oil, yielding a prior austenite grain size of 20 μm. Subsequent tempering was performed at 650°C for one hour. One half of the material was oil quenched after tempering; the other half was taken through a step-cooling procedure of holding for progressively longer times at decreasing temperatures through the temper embrittlement range. The specific details of the two heat-treatments are shown schematically in Fig. 1. The resulting structures are hereafter referred to as unembrittled (oil quenched) and embrittled (step-cooled) respectively.

The loss in toughness which resulted from the embrittling treatment was assessed using plane strain fracture toughness (K_{Ic}) tests at room temperature, using 25.4 mm thick 1-T compact tension specimens. The K_{Ic} value for the unembrittled structure was found to be invalid with respect to A.S.T.M. standards, and accordingly an estimate was computed using an equivalent energy procedure at maximum load.[13] A further estimate was derived by measuring an approximate J_{Ic} value, at initiation of fracture,[14] detected using the electrical potential technique.[16] Uniaxial tensile properties at ambient temperature were

performed using 25.4 mm gage length tensile bars, and cyclic stress-strain data determined from 12.7 mm gage length bars, cycled under strain control, using the incremental-step procedure.[15]

Fatigue crack propagation tests were conducted on 12.7 mm thick 1-T compact tension specimens, cycled, with load control, on a 100 kN electro servo-hydraulic M.T.S. testing machine under sinusoidal tension at load ratios ($R = K_{min}/K_{max}$) of 0.05 and 0.70, where K_{max} and K_{min} are the maximum and minimum stress intensities during each cycle. The cyclic frequency was maintained at 50 Hz. The test environment was laboratory air maintained at a constant temperature of 23°C and a constant relative humidity of 45%. Continuous monitoring of crack length was achieved using the electrical potential method,[16] capable of measurement to within 0.1 mm of absolute crack length, and of detecting changes in crack length of the order 0.01 mm. Numerical differentiation of crack length versus number of cycles data was employed to determine crack growth rates, the data being curve-fitted using finite difference and incremental-step polynomial procedures.[7]

Threshold stress intensities for crack growth (ΔK_o) were calculated in terms of the alternating stress intensity ($\Delta K = K_{max} - K_{min}$) at which no growth could be detected within 10^7 cycles. Since the crack monitoring technique is at least accurate to 0.1 mm, this corresponds to a maximum crack propagation rate of 10^{-8} mm/cycle (4×10^{-10} in/cycle). To avoid residual stress effects, thresholds were approached using a successive reduction in load (of not more than 10 pct reduction in K_{max} at each step) followed by crack growth procedure. Measurements

were taken, at every load level, over increments of crack growth of 1-1.5 mm, representing at least 100 times the maximum plastic zone size generated at the previous load level. Higher growth rate tests were performed under continuous constant load conditions. Plane strain conditions* were maintained in all fatigue tests, except where K_{max} exceeded 80 MPa$\sqrt{m}$.

The grain boundary chemistry of embrittled samples was analyzed using Auger spectroscopy to determine the presence and approximate concentrations of segregated impurities. Specimens were fractured at ambient temperature inside the Auger microprobe under a vacuum of $\sim 10^{-11}$ torr (10^{-8} Pa), and examined using a primary electron beam of 500 μm spot size. Scanning electron microscopy was employed to characterize the fracture morphology of all specimens.

*Based on the criterion that B and $a > 2.5\ (K_{max}/\sigma_y)^2$, where B is the specimen thickness, 'a' the crack length and σ_y is the yield strength.

RESULTS

The ambient temperature mechanical properties of the umembrittled (oil quenched) and temper embrittled (step-cooled) structures are shown in Table 1, where it can be seen that the step-cooling procedure does not lead to any significant loss of strength, measured under both monotonic and cyclic conditions. The cyclic yield stress is 20 pct lower than the monotonic value indicating characteristic cyclic softening of the 650°C tempered structures. Step-cooling does, however, give rise to reduced ductility and, more importantly, to a substantial loss in toughness with the fracture toughness being decreased by approximately 50 pct. The nature of the embrittlement is clearly shown in fractographs of broken K_{Ic} specimens (Fig. 2), indicating 100 pct microvoid coalescence in the unembrittled condition compared to 100 pct intergranular fracture along prior austenite grain boundaries in the embrittled condition. Auger electron microscopy of freshly fractured embrittled samples, before and after extensive sputtering with Ar^+ (Fig. 3), revealed the presence of excess Ni, Mn, P and Si on the grain boundaries. Concentration profiles of these elements adjacent to the boundaries, obtained by successive sputtering and Auger electron spectroscopy, indicated approximate monolayer coverage of Mn, P and Si (Fig. 4). Using appropriate calibrations (see Ref. 17 for details), approximate concentrations of the elements were found to be 6 atomic pct Ni, 4 atomic pct P and 8 atomic pct Si within the first few atomic layers on the grain boundaries (no Mn calibration was obtained). It

appears, therefore, that the severe loss in toughness in 300-M steel, induced by the step-cooling treatment, involves reduced cohesion at grain boundaries from the co-segregation of both alloying elements (Ni and Mn) and impurity elements (P and Si).

The effect of this embrittlement on fatigue crack propagation in moist air is shown in Fig. 5 in terms of the variation of crack growth rate per cycle (da/dN) with the alternating stress intensity (ΔK) for load ratios of 0.05 and 0.70. It is clear that prior temper embrittlement results in a significant reduction in resistance to fatigue crack propagation at both load ratios, particularly as the growth rate is reduced. At growth rates greater than $\sim 10^{-5}$ mm/cycle, the embrittled structure shows only marginally higher growth rates at both load ratios. Furthermore, increasing the load ratio from R = 0.05 to 0.70 does not result in significantly higher propagation rates in either structure. No major differences were observed in the fatigue fracture mechanisms in this region, with both structures exhibiting a transgranular ductile striation mode (Fig. 6), characteristic of martensitic, low alloy steels at intermediate growth rates.[7]

The largest effect of embrittlement on fatigue crack propagation behavior is seen at growth rates less than 10^{-6} mm/cycle, where the alternating stress intensity (ΔK) approaches a threshold value (ΔK_o). Growth rates in the embrittled structure become over an order of magnitude higher than in the umembrittled structure. Furthermore, the value of the threshold ΔK_o is significantly reduced by embrittlement, from 8.5 to 6.2 MPa$\sqrt{m}$ at R = 0.05, and from 3.7 to 2.7 MPa$\sqrt{m}$ at R = 0.70,

representing a reduction of almost 30 pct in each case. It is also noticable that growth rates are increasingly sensitive to the load ratio as the threshold is approached. Fracture surfaces in this region are shown in Fig. 7, where it can be seen that, in embrittled samples, significant amounts of intergranular fracture are present. The proportion of intergranular facets was found to vary with stress intensity, increasing from around 5 pct near ΔK_o to approximately 20 pct at ΔK = 10 MPa$\sqrt{m}$ (at R = 0.05) and then virtually disappearing above $\Delta K \gtrsim 15$ MPa$\sqrt{m}$ (Fig. 8). No evidence of intergranular fracture could be detected at any stress intensity in unembrittled samples (Fig. 7a and 8a).

It is thus apparent that prior temper embrittlement can substantially reduce fatigue crack propagation resistance at low (near-threshold) growth rates in humid air, and that this lowered resistance is coincident with a transition from purely transgranular to an intergranular plus transgranular mode of fatigue fracture.

DISCUSSION

i) General Nature of Embrittlement in 300-M Steel

The temper embrittlement of 300-M steel, induced by step-cooling after tempering at 650°C, has been shown to result from a build-up of Ni, Mn, P and Si in prior austenite grain boundaries. The segregation of both alloying and impurity elements in this steel is consistent with a recent theory of temper embrittlement, proposed by Güttmann[18] and experimentally verified by McMahon and co-workers.[17,19,20] Impurity elements, such as P, interact attractively with alloying elements, such as Ni and Mn, but retain their mobility. Co-segregation of both alloying and impurity elements can thus take place to grain boundaries, where interface cohesion is reduced by the presence of the impurity elements. The presence of Cr can further promote this segregation,[19] either by acting as a catalyst or by segregating itself.* The kinetics of embrittlement in P-containing Ni-Cr steels has been shown to be consistent with equilibrium (Gibbsian) segregation[21] of P, controlled by P diffusion, and co-segregation of Ni. Ni enrichment can further occur in grain boundaries since this element is rejected by Cr-rich carbides which grow in the boundaries during step-cooling.[6,20] Moreover, there is now clear evidence of additional pre-transformation segregation of P in the austenitic phase, either prior to, or during quenching after austenitization.[22,23,3] The presence of significant amounts of

*Chromium segregation results are ambiguous because of experimental difficulties with Auger spectroscopy. The difficulty in detecting this element in grain boundaries is due to interference from the oxygen peak and from Cr in Cr-rich boundary carbides.[19]

Si in grain boundaries in the present steel suggests a possible embrittling effect from this impurity element. Several other authors have observed the segregation of Si[9,10] and suggested that it may act to lower grain boundary cohesion,[24,22,9,10] but the specific details of embrittlement by this element (if indeed it does cause embrittlement) remain to be determined. Hence, the temper embrittlement of 300-M steel, induced by step-cooling from 650°C, appears to result from the co-segregation of alloying elements (Ni and Mn) and impurity elements (P and Si) to prior austenite grain boundaries where P, and possibly Si, reduce cohesion sufficiently to cause 100 pct brittle intergranular separation and a corresponding severe loss in toughness.

ii) Effect of Embrittlement on Fatigue Crack Propagation

The magnitude of the effect of embrittlement on fatigue crack propagation has been found to be different for different ranges of growth rates. It is possible to characterize these ranges in terms of their dependence on the alternating stress intensity (ΔK), as shown schematically in Fig. 9. For the intermediate range of growth rates (regime B), where da/dN is typically between 10^{-5}-10^{-3} mm/cycle, the propagation rate can be expressed in terms of the Paris power law equation,[25] such that

$$\frac{da}{dN} = C\Delta K^m , \qquad (1)$$

where 'C' and 'm' are scaling constants, and 'm' takes values typically between 2 and 4. In this range, the growth mechanism in steels is primarily striation growth, and propagation rates are largely insensitive to microstructure and load ratio (mean stress).[26,7,27] At

higher growth rates (regime C), where K_{max} approaches K_{Ic}, the fracture toughness, superimposed 'static' fracture modes (ie. cleavage, intergranular and fibrous fracture)* can occur during striation growth, and the propagation rate becomes markedly sensitive to microstructure and load ratio.[26,7,27] Similarly at low growth rates less than $10^{-5} - 10^{-6}$ mm/cycle (regime A), where ΔK approaches a threshold, ΔK_o, a strong dependence on microstructure and load ratio is again observed. The explantion for this dependence, however, is still a subject of some controversy, involving conflicting viewpoints based on environmental[27,32,33] and crack closure concepts.[28-31]

The present study has examined the effect of prior temper embrittlement on fatigue crack propagation behavior at lower and intermediate growth rates (regimes A and B) and, whereas it is clear that a strong effect exists in regime A, growth rates in regime B are far less affected. Previous research[7] at high growth rates, greater than 10^{-4} mm/cycle (regime C), has shown that prior temper embrittlement can severely reduce fatigue crack propagation resistance in this range. Here, brittle intergranular cracking occurs during striation growth in embrittled material because of its low toughness. This causes a substantial acceleration in growth rate compared to unembrittled material and,

---

*Such fracture mechanisms are generally regarded as tensile stress-controlled, or in the case of fibrous fracture, controlled by the hydrostatic component of stress. Increasing the load ratio raises K_{max} with respect to ΔK, and therefore leads to a greater contribution from such modes and consequently increases the growth rate. The onset of "static mode-assisted" propagation in regime C is thus dependent on the toughness and occurs as K_{max} approaches K_{Ic}.[7,27]

since intergranular cracking is a tensile stress-controlled mode of fracture,[7] growth rates in the embrittled steel become markedly sensitive to load ratio.

At intermediate growth rates, however, the value of K_{max} is small compared with K_{Ic} and thus static fracture modes do not generally occur during fatigue crack propagation in this regime. The loss in toughness, arising from embrittlement, is thus not so important in influencing growth rate behavior. The present investigation has shown that the mechanism of growth is similar in both unembrittled and embrittled samples, i.e. striation growth (Fig. 6) and this is consistent with the small influence of prior embrittlement observed. Begley and Toolin[34] similarly observed little influence of temper embrittlement on fatigue crack propagation in a Ni-Cr-Mo-V steel at such intermediate growth rates (3×10^{-5} to 5×10^{-4} mm/cycle). Furthermore, the lack of a significant effect of load ratio on propagation rates in this region is consistent with a striation mechanism of growth.[7,26,27]

As the growth rate is reduced below 10^{-6} mm/cycle in regime A, however, the present results show i) a marked dependence of the growth rate on load ratio, and ii) that prior temper embrittlement leads to a severe deterioration in resistance to fatigue crack propagation (in the form of increased growth rates and a lower threshold), coincident with the occurrence of intergranular fracture in embrittled samples. Effects of embrittlement and load ratio thus principally affect near-threshold growth rates and are far less important at higher propagation rates in the intermediate range. These results can be interpretated in

terms of a model[27] relating the contributions to fatigue crack growth due to i) embrittlement induced by impurity segregation (temper embrittlement) and ii) embrittlement arising from the presence of hydrogen atoms, evolved from crack tip surface reactions with vapor in the moist air environment (hydrogen embrittlement).

Model for Near-Threhold Fatigue Crack Growth

Following Weiss and Lal,[35] a model for fatigue crack propagation is considered based on the assumption that the crack advance per cycle (da/dN) represents the distance ahead of the crack tip where the nominal stress exceeds a certain critical fracture stress (σ_F), such that

$$\frac{da}{dN} = \frac{\Delta K^2}{\pi \sigma_F^2} - \frac{\rho^*}{2} \quad , \tag{2}$$

where ρ^* is the Neuber micro-support constant representing the effective radius of the crack.* For the limiting conditions of crack growth near the threshold, the local tensile stress (σ_{yy}) must exceed σ_F over a distance larger than ρ^* and hence, at the threshold, Weiss and Lal[35] propose $da/dN = \rho^*$, viz.

$$\Delta K_o = \sqrt{\frac{3}{2} \pi \rho^*} \cdot \sigma_F \quad . \tag{3}$$

Since the presence of impurity elements in grain boundaries will lead to a reduction in the cohesive strength, it can be considered that prior temper embrittlement lowers this critical fracture stress (σ_F) by an amount $\Delta\sigma_1$ due to impurities, thus

*The significance of the ρ^* parameter, and its relationship to microstructure, is described in greater detail in references 27 and 35.

$$\frac{da}{dN} = \frac{\Delta K^2}{\pi(\sigma_F - \Delta\sigma_I)^2} - \frac{\rho^*}{2} \quad . \tag{4}$$

In a moist air environment, cyclic stressing will lead to the production of chemically reactive surface at the crack tip, where atomic hydrogen can be evolved from water vapor by reactions[36] of the type

$$\begin{aligned} Fe + H_2O &\rightleftharpoons FeOH^+ + H^+ + 2e \\ 2H^+ + 2e &\rightleftharpoons 2H \quad . \end{aligned} \tag{5}$$

The stress gradient ahead of the crack tip then drives adsorbed hydrogen atoms into the lattice where they accumulate in the region of highest dilatation (the point of maximum hydrostatic tension) and further lower the cohesive strength.[37] If the reduction in cohesive strength due to hydrogen is taken as $\Delta\sigma_H$, then the combined influence of impurities and hydrogen effects (assuming initially that they are simply additive) on fatigue crack growth can be represented by

$$\frac{da}{dN} = \frac{\Delta K^2}{\pi(\sigma_F - \Delta\sigma_I - \Delta\sigma_H)^2} - \frac{\rho^*}{2} \quad , \tag{6}$$

where the threshold is given by

$$\Delta K_o = \sqrt{\frac{3}{2}\pi\rho^*} \cdot (\sigma_F - \Delta\sigma_I - \Delta\sigma_H) \quad . \tag{7}$$

Following the procedure of McMahon et al.,[10] it is possible to derive expressions for the terms $\Delta\sigma_I$ and $\Delta\sigma_H$. The reduction in cohesive strength due to impurities ($\Delta\sigma_I$) can be related to a reduction ($\Delta\gamma$) in

grain boundary surface energy (γ_o), due to the presence of a solute, ie.

$$\sigma_F - \Delta\sigma_I \simeq \sigma_c \left(1 - \frac{\Delta\gamma}{\gamma_o}\right)^{1/2} . \qquad (8)$$

where σ_c is the theoretical cohesive strength. Based on the data of Hondros[38] for P in α-iron, McMahon et al.[10] estimate a $\Delta\sigma_I$ of 30 pct, which, as they state, is a substantial reduction.

The reduction in cohesive strength due to hydrogen ($\Delta\sigma_H$) can be considered to be proportional to the local concentration of hydrogen in the region of maximum hydrostatic tension (C_H), and can be expressed by[39]

$$\Delta\sigma_H = \alpha C_H \simeq \alpha C_o \cdot \exp\left(\frac{\bar{V}\cdot\bar{\sigma}}{R_o T}\right) , \qquad (9)$$

where C_o is the equilibrium concentration of hydrogen in the unstressed lattice, α an unknown constant, $\bar{V}$ the partial molar volume of hydrogen in iron (2 cm^3/mole), $\bar{\sigma}$ the hydrostatic tension, R_o the Gas Constant, and T the absolute temperature. Substituting an expression for the maximum hydrostatic tension ($\bar{\sigma}$),[40,27] Eq. (9) becomes

$$\Delta\sigma_H = \alpha C_o \exp\left[\frac{\bar{V}}{R_o T}\left(\sigma_y + 2\alpha_1 K_{max}\right)\right] , \qquad (10)$$

where σ_y is the yield strength, K_{max} the maximum stress intensity of the fatigue loading cycle and α_1 an empirical constant equal to 2 $in^{-1/2}$. Utilizing the above equations it is possible to rationalize the present results for the fatigue crack propagation behavior of unembrittled and temper embrittled 300-M in moist air. Effects of prior temper

embrittlement and load ratio are now considered in turn.

i) Effects of Prior Temper Embrittlement

It is clear that the reduction in cohesion due to the presence of impurities ($\Delta\sigma_I$) should lead to higher crack propagation rates from Eq. (4), and this is consistent with experimental results in Fig. 5 for near-threshold and intermediate growth rates. However, at near-threshold growth rates, there will be a further reduction in cohesive strength due to the presence of hydrogen atoms ($\Delta\sigma_H$). This environmental effect will be less apparent (at a given frequency) as the growth rate is increased (i.e. at intermediate growth rates), since at higher crack velocities, there is insufficient time for the permeation of atomic hydrogen into the crack tip region. Thus, one might expect a larger influence of prior temper embrittlement at near-threshold growth rates because of reduced cohesion from both impurities and hydrogen atoms, as experimentally observed in Fig. 5. This suggests a synergistic relationship between impurity and hydrogen effects, where the presence of the impurity atom in grain boundaries could raise the local concentration of hydrogen (C_o), due to an attractive interaction between impurity and hydrogen atoms.[10] There is a further possibility that, at chemically active sites (eg. grain boundaries) on freshly exposed surface at the crack tip where hydrogen is initially adsorbed from the environment, the presence of impurity atoms in embrittled material can further raise the local value of C_o by retarding the re-combination of atomic hydrogen.[11] These effects are consistent

with higher fatigue crack propagation rates (Eq. 6) and lower threshold values (Eq. 7) observed in embrittled material at near-threshold growth rates, and a much smaller influence of temper embrittlement observed at intermediate growth rates.

ii) Effect of Load Ratio

The reduction in cohesion due to hydrogen ($\Delta\sigma_H$) is not merely a function of C_o but also dependent on the enrichment of hydrogen concentration (C_H/C_o) in the region of maximum dilatation ahead of the crack tip. This enrichment is a function of the magnitude of the hydrostatic tension (Eq. 9), which can be raised by increasing material strength, σ_y*, or by increasing the maximum stress intensity, K_{max} (Eq. 10). Thus, as the load ratio, R, is raised, the corresponding increase in K_{max} (= $\Delta K/1-R$) leads to a greater local concentration of hydrogen (C_H) which reduces cohesion, and hence, to an increase in growth rate (Eq. 6) and a decrease in ΔK_o (Eq. 7). Additionally, the effect of a larger value of K_{max} is to raise the plastic stress gradient ahead of the crack tip, thus providing a greater driving force for hydrogen transport into the region of maximum triaxiality. Therefore, one expects an influence of load ratio on fatigue crack propagation, but because this influence arises from the environmental effect of hydrogen,

---

*It has been shown elsewhere[27] that higher near-threshold fatigue crack propagation rates and lower threshold values result when the (cyclic) yield strength of 300-M steel is raised (Fig. 10), and this is consistent with an increasing susceptibility to hydrogen embrittlement with increase in strength.[40]

it should decrease i) at higher growth rates (regime B), when hydrogen diffusion ahead of the crack tip can no longer keep pace with the crack velocity,* and ii) at near-threshold growth rates for tests in inert environments. This is consistent i) with the present results (Fig. 5) which show the influence of load ratio to be considerably smaller at intermediate growth rates compared to near-threshold behavior, and ii) with the data of Beevers and co-workers[32,33] which indicate that the load ratio has a negligible effect on near-threshold growth rates measured *in vacuo*. Contrary to this, Paris and co-workers[28-30] have suggested that the nature of the environment has little influence on near-threshold behavior, based on tests in air and argon of unspecified purity. However, it has been pointed out that the argon atmosphere used in the latter experiments was not sufficiently inert to remove all traces of moisture.[32]

Another interpretation of the influence of load ratio on low fatigue crack growth rates has been proposed,[28-31] based on the effect of crack closure.[41] The concept of crack closure relies on the fact that, as a result of plastic deformation left in the wake of a growing fatigue crack, it is possible that some closure of the crack surfaces may occur during the loading cycle. Since the crack is unable to propagate while it remains closed, the net effect of closure is to

---

*Load ratio effects can re-appear at even higher propagation rates (regime C) due to the occurrence of static modes of fracture during fatigue crack growth.[7,27]

reduce the applied ΔK value* to some lower effective value (ΔK_{eff}) actually experienced at the crack tip. As the load ratio is increased, the crack is assumed to remain open for a larger portion of the cycle, thus increasing the value of ΔK_{eff} and hence the growth rate. This concept has been utilized to explain the effect of load ratio on near-threshold growth in low strength steels,[28,29] titanium[30] and aluminum[31] alloys, but with little or no experimental verification. Furthermore, closure arguments cannot account for the fact that the effect of load ratio in steels is minimal at intermediate growth rates (regime B), where closure is equally likely to occur. Electrical potential measurements during the present investigation were unable to detect any crack closure near the threshold, except below the minimum stress intensity (K_{min}) of the loading cycle. Although these results cannot be regarded as conclusive, since measurements of fracture surface contact in air are likely to be masked by the presence of oxide scale, they are nevertheless in support of previous observations[42,43] that closure is essentially a surface (plane stress) effect, having a negligible consequence on crack growth under plane strain conditions. This is further supported by the results of Shih and Wei,[44] which indicate that the amount of crack closure near the threshold (where plane strain conditions invariably are present) can be considered minimal. There is a further possibility that closure and environmental effects are interrelated, since the proportion of closure has been

*Applied ΔK refers to the value of the alternating stress intensity computed from applied loads and crack length measurements.

observed to be influenced by the nature of the environmental species present.[45-48] These results indicate, however, that the closure level in inert environments is greater than[45-47] (or at least equal to[48]) the closure level in air. Since the effect of load ratio at low growth rates is much smaller in such inert environments,[32-33] it seems unlikely that crack closure is primarily responsible for the marked dependence of near-threshold growth rates on the load ratio.

It is thus concluded that although extensive data on the effect of environment and crack closure on near-threshold fatigue crack propagation are not available at this time, the present results on the influence of impurity-induced embrittlement and load ratio can be usefully rationalized in terms of the contribution to fatigue crack growth in steels from the environmental influence of hydrogen. This can occur with fatigue loading at stress intensities less than the threshold for hydrogen-assisted cracking under monotonic loading (K_{TH}), because fresh surface at the crack tip, where atomic hydrogen can be evolved, is continually renewed by cyclic stressing.

CLOSING REMARKS

It has been experimentally shown that temper embrittlement in 300-M steel, induced by step-cooling, involves the build-up of both alloying (Ni and Mn) and impurity elements (P and Si) in prior austenite grain boundaries, and that this embrittlement can reduce resistance to fatigue crack propagation in moist air. The large effect on fatigue resistance at near-threshold growth rates, compared to the much smaller effect at intermediate growth rates, has been interpretated in terms of the interaction between segregated impurity atoms and hydrogen atoms evolved from crack tip surface reactions with water vapor in moist air. The fact that a larger influence of prior temper embrittlement has been observed at lower growth rates, where there is likely to be a greater contribution from environmentally-assisted crack growth, suggests that the impurity-hydrogen interactions in this case are synergistic, although other authors[9,10] have indicated that they may be additive (from studies of hydrogen-induced cracking under monotonic loading). Precise resolution of this question requires i) evaluation of the potency of various impurities on hydrogen embrittlement compared to temper embrittlement,* ii) *in situ* identification of impurities on environmentally-induced fracture surfaces,[50] and iii) assessment of the effect of impurity-induced embrittlement on fatigue crack growth *in vacuo*. Similarly, verification of the proposed model for the effect

*If the interactions are additive, then the ranking of the potency of various impurities will be identical for temper and hydrogen embrittlement.[49]

of load ratio on near-threshold fatigue crack growth behavior based on the environmental influence of hydrogen must await more extensive data on low fatigue crack growth rates ($< 10^{-6}$ mm/cycle) under carefully controlled inert atmospheres. In view of the conflicting results[30,32,33] observed in such environments, experiments are required in both inert argon and high vacuum conditions. Finally, the influence of crack closure on fatigue crack growth, particularly under plane strain conditions and in various environments, needs further evaluation in the light of its significance to near-threshold behavior.

CONCLUSIONS

From a study of the effect of temper embrittlement on fracture and fatigue crack propagation in 300-M high strength steel, the following conclusions can be made:

1) Step-cooling, as opposed to oil quenching, after tempering at 650°C, results in a severe loss of toughness (temper embrittlement), concurrent with a transition from 100 pct fibrous to 100 pct intergranular mode of fracture.

2) Based on Auger spectroscopy results, the temper embrittlement of 300-M steel is attributed to the co-segregation of alloying elements (Ni and Mn) and impurity elements (P and Si) to prior austenite grain boundaries, where P (and possibly Si) are considered to reduce the cohesive strength.

3) The effect of this embrittlement on fatigue crack propagation in moist air is to increase crack growth rates, particularly at lower stress intensities.

4) At intermediate growth rates (10^{-5} - 10^{-3} mm/cycle) the effect of prior temper embrittlement is small. Propagation rates in both unembrittled and embrittled material are similar, and only weakly dependent on the load ratio, consistent with the striation mode of growth observed.

5) At near-threshold growth rates ($< 10^{-5}$ - 10^{-6} mm/cycle), embrittled material exhibits significantly higher propagation rates, 30 pct reduction in threshold stress intensity (ΔK_o) values, and intergranular facets on fatigue fracture surfaces. Propagation rates

(and threshold values) are strongly dependent on the load ratio.

6) Evidence of crack closure could not be detected near the threshold, except below the minimum stress intensity (K_{min}) of the loading cycle.

7) The effect of prior temper embrittlement is ascribed to the combined influence of hydrogen atoms, arising from the moist air environment at low growth rates (hydrogen embrittlement), and segregated impurity atoms, both of which are considered to lower the cohesive stress for crack propagation.

8) The effect of load ratio on crack propagation behavior is consistent with the environmental influence of hydrogen at low growth rates, and apparently inconsistent with crack closure concepts.

ACKNOWLEDGEMENTS

The research was conducted under the auspices of the U.S. Energy Research and Development Administration through the Materials and Molecular Research Division of the Lawrence Berkeley Laboratory. The author acknowledges the Miller Institute for Basic Research in Science of the University of California for the award of a University Miller Research Fellowship. Particular thanks are due to Drs. S. K. Banerji and H. C. Feng for performing the Auger spectroscopy, Professor C. J. McMahon and Dr. R. M. Horn for many helpful discussions, and Professors E. R. Parker and V. F. Zackay for their continued help and encouragement.

REFERENCES

1. J. R. Low, Jr.: in Fracture of Engineering Materials, ASM, 1964, p.127.

2. J. R. Low, Jr., D. F. Stein, A. M. Turkalo and R. P. Laforce: Trans TMS-AIME, 1968, vol. 242, p.14.

3. H. Ohtani and C. J. McMahon, Jr.: Acta Met., 1975, vol. 23, p. 377.

4. J. M. Capus: Rev. Met., 1959, vol. 56, p.181.

5. E. B. Kula and A. A. Anctil: J. Materials, 1969, vol.4, p.817.

6. J. R. Rellick and C. J. McMahon, Jr.: Met. Trans., 1974, vol. 5, p.2439.

7. R. O. Ritchie and J. F. Knott: Acta Met., 1973, vol. 21, p. 639.

8. R. Bruscato: Weld. J. Res. Suppl., 1970, vol. 49, p. 148-S.

9. K. Yoshino and C. J. McMahon, Jr: Met. Trans., 1974, vol. 5, p. 363.

10. C. J. McMahon, Jr., C. L. Briant and S. K. Banerji: Proc. Fourth Int. Conf. on Fracture, Waterloo, Canada, June 1977.

11. R. Viswanathan and S. J. Hudak: in Effect of Hydrogen on Behavior of Materials (eds. A. W. Thompson and I. M. Bernstein), p.262, 1975. The Metallurgical Society of AIME.

12. R. P. Wei and J. D. Landes: Materials Research and Standards, 1969, vol. 9, p.25.

13. F. J. Witt: Fourth National Symposium on Fracture Mechanics, Carnegie-Mellon University, Aug. 1970.

14. J. D. Landes and J. A. Begley: Westinghouse Scientific Paper 76-1E7-JINTF-P3, May 1976, Westinghouse Scientific Laboratories, Pittsburg, PA.

15. R. W. Landgraf, J-D. Morrow, and T. Endo: J. Materials, 1969, vol. 4, p. 176.

16. R. O. Ritchie, G. G. Garrett and J. F. Knott: Int. J. Fracture Mechanics, 1971, vol. 7, p. 462.

17. H. Ohtani, H. C. Feng, C. J. McMahon, Jr., and R. A. Mulford: Met. Trans. A, 1976, vol. 7A, p. 87.

18. M. Guttmann: Surface Sci., 1975, vol. 53, p.213.

19. R. A. Mulford, C. J. McMahon, Jr., D. P. Pope, and H. C. Feng: Met. Trans. A., 1976, vol. 7A, p. 1183.

20. C. J. McMahon, Jr., E. Furubayashi, H. Ohtani and H. C. Feng: Acta Met., 1976, vol. 24, p. 695.

21. D. McLean: in Grain Boundaries in Metals, Oxford University Press, London, 1957.

22. B. J. Schulz and C. J. McMahon, Jr.: in Temper Embrittlement of Alloy Steels, p. 104, ASTM STP 499, ASTM Philadelphia, 1972.

23. G. Clark, R. O. Ritchie and J. F. Knott: Nature Phys. Sci., 1972, vol. 239, p. 104.

24. W. Steven and K. Balajiva: JISI, 1959, vol. 193, p. 141.

25. P. C. Paris and F. Erdogan: J. Basic Engineering, Trans. ASME Series D, 1963, vol. 85, p. 528.

26. C. E. Richards and T. C. Lindley: Eng. Fract. Mech., 1972, vol. 4, p. 951.

27. R. O. Ritchie: J. Engineering Materials and Technology, Trans. ASME Series H, 1977 in press, (Lawrence Berkeley Laboratory, Report No. LBL-5496, Oct. 1976, University of California).

28. P. C. Paris, R. J. Bucci, E. T. Wessel, W. G. Clark, and T. R. Mager: in Stress Analysis and Growth of Cracks, p. 141, ASTM STP 513, ASTM Philadelphia 1972.

29. R. J. Bucci, W. G. Clark, Jr., and P. C. Paris: ibid., p. 177.

30. R. J. Bucci, P. C. Paris, R. W. Hertzberg, R. A. Schmidt, and A. F. Anderson: ibid, p.125.

31. R. A. Schmidt and P. C. Paris: in Progress in Flaw Growth and Fracture Toughness Testing, p.79, ASTM STP 536, ASTM Philadelphia 1972.

32. P. E. Irving and C. J. Beevers: Met. Trans., 1974, vol. 5, p. 391.

33. R. J. Cooke, P. E. Irving, G. S. Booth, and C. J. Beevers: Eng. Fract. Mech., 1975, vol. 7, p. 69.

34. J. A. Begley and P. R. Toolin: Int. J. of Fracture, 1973, vol. 9, p. 243.

35. V. Weiss and D. N. Lal: Met. Trans., 1974, vol. 5, p. 1946.

36. T. Misawa: Corrosion Sci., 1973, vol. 13, p. 659.

37. A. R. Troiano: Trans. ASM, 1960, vol. 52, p. 54.

38. E. D. Hondros: Proc. Royal Soc. A, 1965, vol. 286, p. 479.

39. R. A. Oriani and P. H. Josephic: Acta Met., 1974, vol. 22, p. 1065.

40. W. W. Gerberich and Y. T. Chen: Met. Trans. A, 1975, vol. 6A, p. 271.

41. W. Elber: in Damage Tolerance in Aircraft Structures, p. 230, ASTM STP 486, ASTM, Philadelphia, 1971.

42. T. C. Lindley and C. E. Richards, Mater. Sci. Eng. 1974, vol. 14, p. 281.

43. F. J. Pitoniak, A. F. Grandt, L. T. Montulli, and P. F. Packman: Eng. Fract. Mech., 1974, vol. 6, p. 663.

44. T. T. Shih and R. P. Wei: ibid., 1974, vol. 6, p. 19.

45. O. Buck, J. D. Frandsen, and H. L. Marcus: ibid., 1975, vol. 7, p. 167.

46. P. E. Irving, J. L. Robinson, and C. J. Beevers: ibid., 1975, vol. 7, p. 619.

47. P. E. Irving, J. L. Robinson, and C. J. Beevers: Int. J. Fracture, 1973, vol. 9, p. 105.

48. V. Bachman and D. Munz: ibid., 1975, vol. 11, p. 713.

49. C. J. McMahon, Jr.: Mater. Sci. Eng., 1977, vol. 25, p. 233.

50. R. P. Wei and G. W. Simmons: Scripta Met., 1976, vol. 10, p. 153.

TABLE CAPTIONS

Table 1. Ambient temperature mechanical properties of 300-M steel in the unembrittled and temper embrittled condition.

Table 1. Ambient Temperature Mechanical Properties of 300-M Steel in the Unembrittled and Temper Embrittled Condition.

Code	Austenitizing Treatment	Temper	Monotonic Yield Stress[1] (MPa)	U.T.S. (MPa)	True Fracture Strain	Reduction in Area (pct)	K_{Ic} (MPa$\sqrt{m}$)	Cyclic Yield Stress[1] (MPa)	Prior Austenite Grain Size (μm)
umembrittled	870°C (1 hr) oil quenched	650°C (1 hr) oil quenched	1074	1186	0.81	56	185[2] 152[3]	861	20
embrittled	870°C (1 hr) oil quenched	650°C (1 hr) step-cooled[4]	1070	1179	0.73	52	79.6	858	20

[1]Yield stress measured by 0.2% offset.

[2]Invalid K_{Ic} result, estimated using equivalent energy procedure at maximum load.[13]

[3]Invalid K_{Ic} result, estimated using J_{Ic} approach at initiation.[14]

[4]Step-cooling procedure described in Fig. 1.

FIGURE CAPTIONS

Fig. 1. Schematic representation of heat treatments employed.

Fig. 2. Fracture surfaces from K_{Ic} specimens showing a) 100 pct microvoid coalescence in unembrittled material, and b) 100 pct intergranular cracking in temper embrittled material.

Fig. 3. Auger spectra from an intergranular fracture surface of temper embrittled 300-M steel, immediately after fracture (upper curve) and after extensive Ar^+ ion sputtering (lower curve).

Fig. 4. Concentration profiles of segregated elements in temper embrittled 300-M steel, showing concentration distributions in regions adjacent to the grain boundary.

Fig. 5. Variation of fatigue crack growth rate (da/dN) in moist air with alternating stress intensity (ΔK) at R = 0.05 and 0.70 for umembrittled and temper embrittled 300-M steel. ΔK_o is the threshold stress intensity below which crack propagation cannot be detected.

Fig. 6. Ductile striation growth at intermediate propagation rates in a) unembrittled and b) temper embrittled 300-M steel. (ΔK = 30 MPa$\sqrt{m}$, R = 0.05. Arrow indicates general direction of crack propagation).

Fig. 7. Morphology of fatigue fracture at near-threshold crack growth rates at ΔK = 9.5 MPa$\sqrt{m}$ (R = 0.05) in 300-M steel showing a) ductile transgranular mechanism in unembrittled material, and b) segments of intergranular fracture (I) in temper embrittled material. (Arrow indicates general direction of crack propagation).

Fig. 8. Morphology of fatigue fracture at ΔK = 15 MPa$\sqrt{m}$ (R=0.05) in 300-M steel in a) unembrittled and b) temper embrittled material. (Arrow indicates general direction of crack propagation).

Fig. 9. Schematic diagram showing the primary fracture mechanisms and associated fatigue behavior consistent with the sigmoidal variation of fatigue crack propagation rate (da/dN) with alternating stress intensity (ΔK). ΔK_o is the threshold stress intensity for crack growth, K_c the stress intensity at final failure.

Fig. 10. Influence of cyclic strength on the threshold for fatigue crack growth (ΔK_o), at R=0.05 and 0.70, for quenched and tempered 300-M steel, showing additional effect of temper embrittlement, induced by step-cooling.

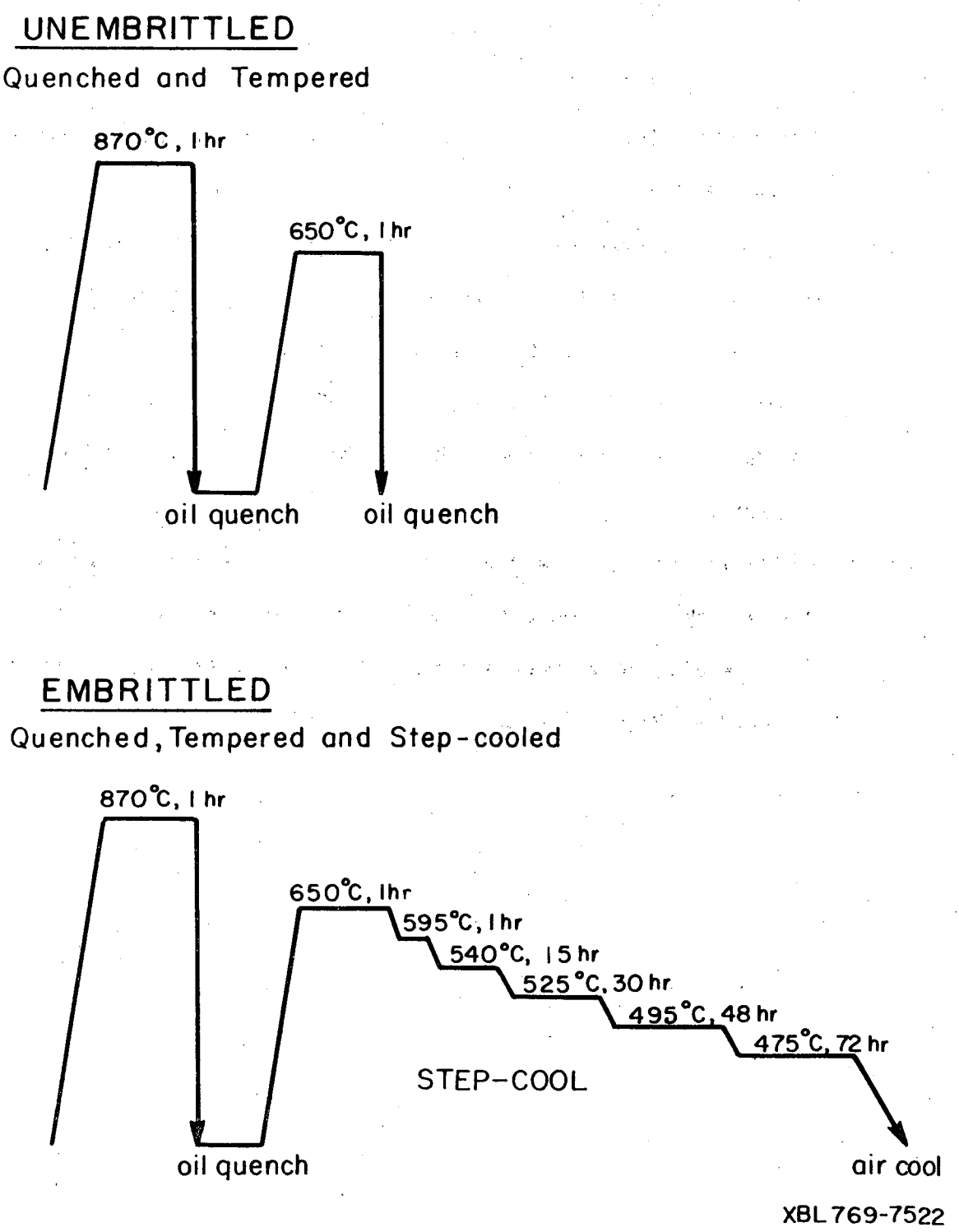

Fig. 1. Schematic representation of heat treatments employed.

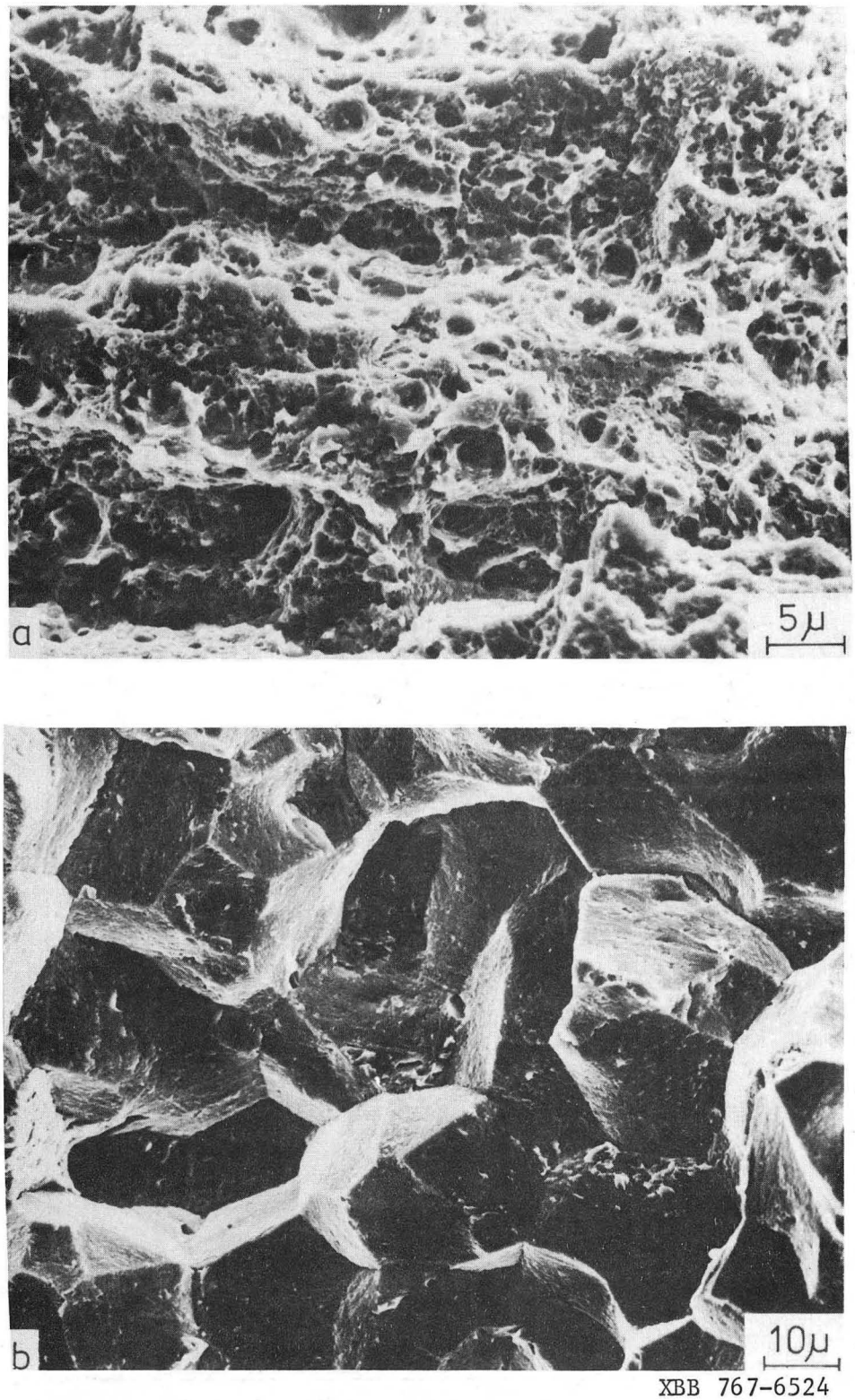

XBB 767-6524

Fig. 2. Fracture surfaces from K_{Ic} specimens showing a) 100 pct microvoid coalescence in unembrittled material, and b) 100 pct intergranular cracking in temper embrittled material.

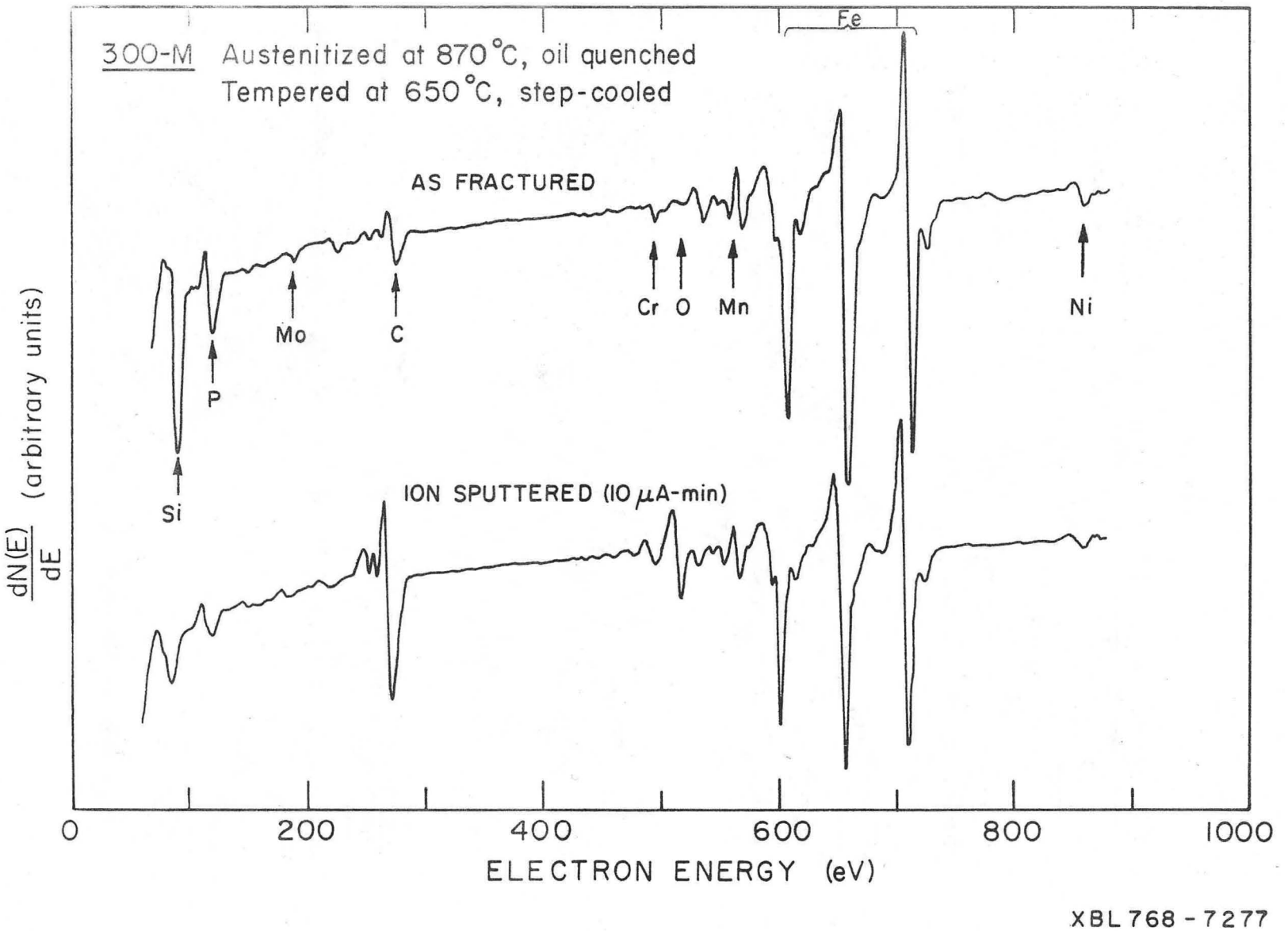

Fig. 3. Auger spectra from an intergranular fracture surface of temper embrittled 300-M steel, immediately after fracture (upper curve) and after extensive Ar^+ ion sputtering (lower curve).

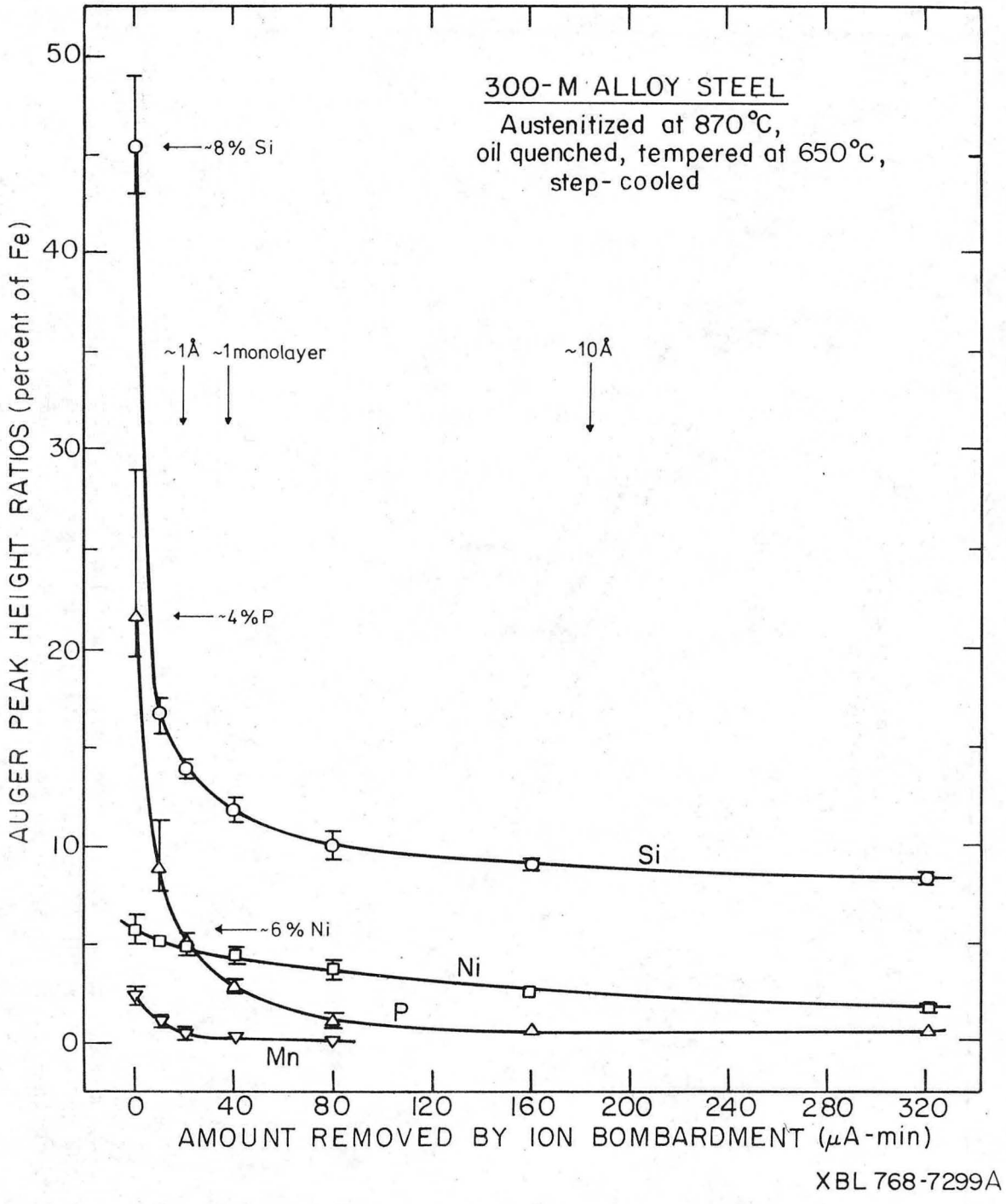

Fig. 4. Concentration profiles of segregated elements in temper embrittled 300-M steel, showing concentration distributions in regions adjacent to the grain boundary.

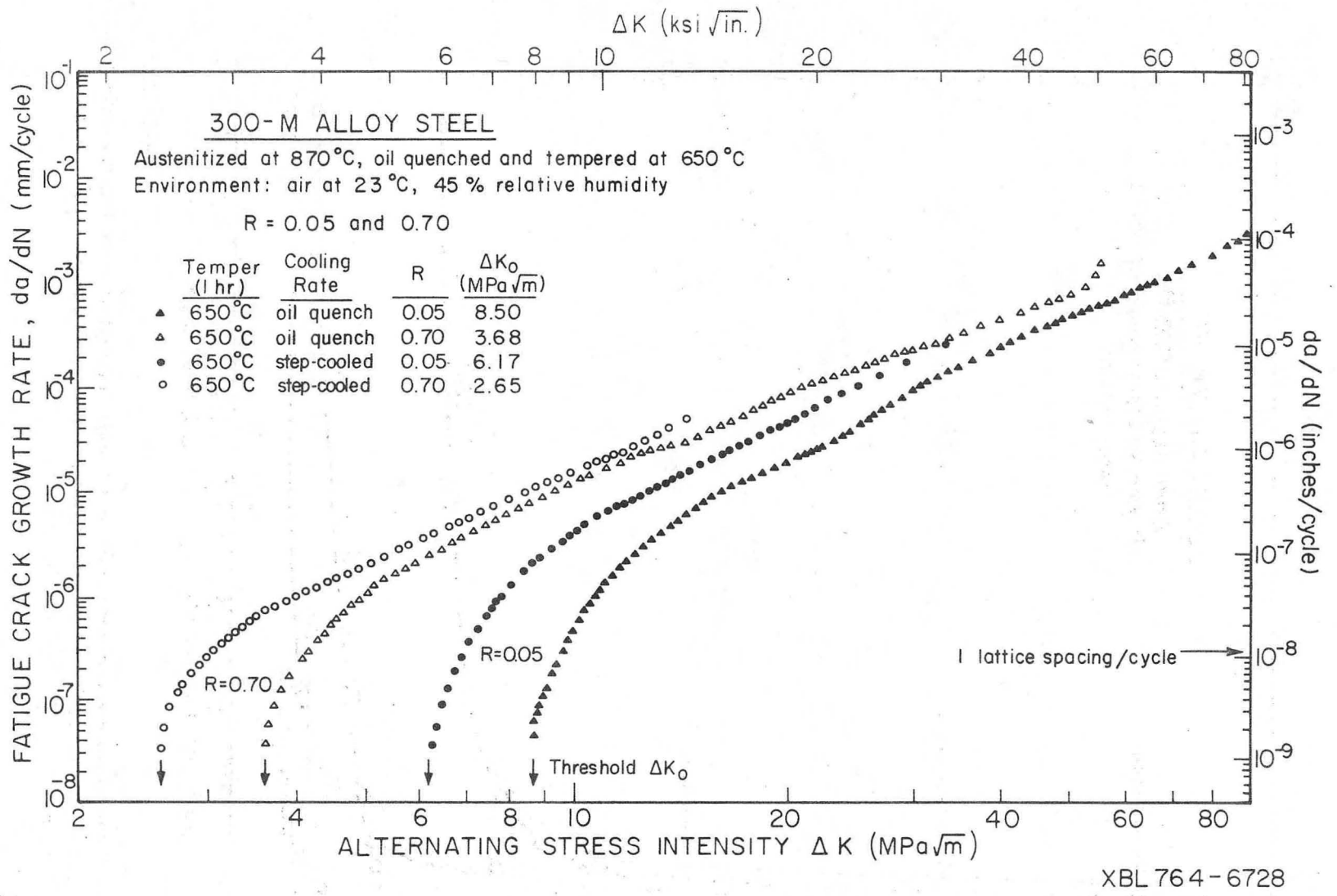

Fig. 5. Variation of fatigue crack growth rate (da/dN) in moist air with alternating stress intensity (ΔK) at R=0.05 and 0.70 for unembrittled and temper embrittled 300-M steel. ΔK_o is the threshold stress intensity below which crack propagation cannot be detected.

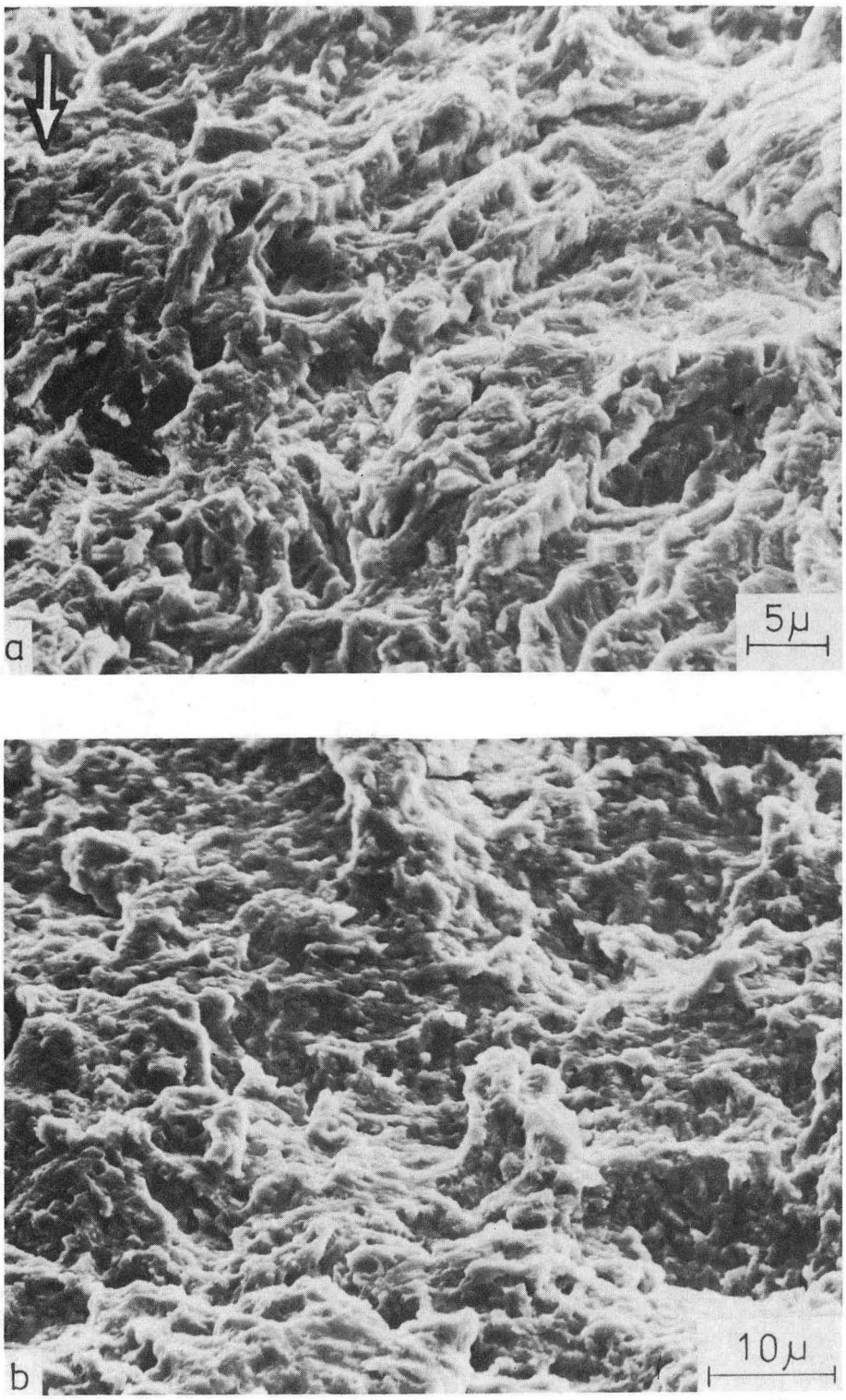

XBB 7610-9634

Fig. 6. Ductile striation growth at intermediate propagation rates in a) unembrittled and b) temper embrittled 300-M steel. (ΔK = 30 MPa$\sqrt{m}$, R = 0.05. Arrow indicates general direction of crack propagation).

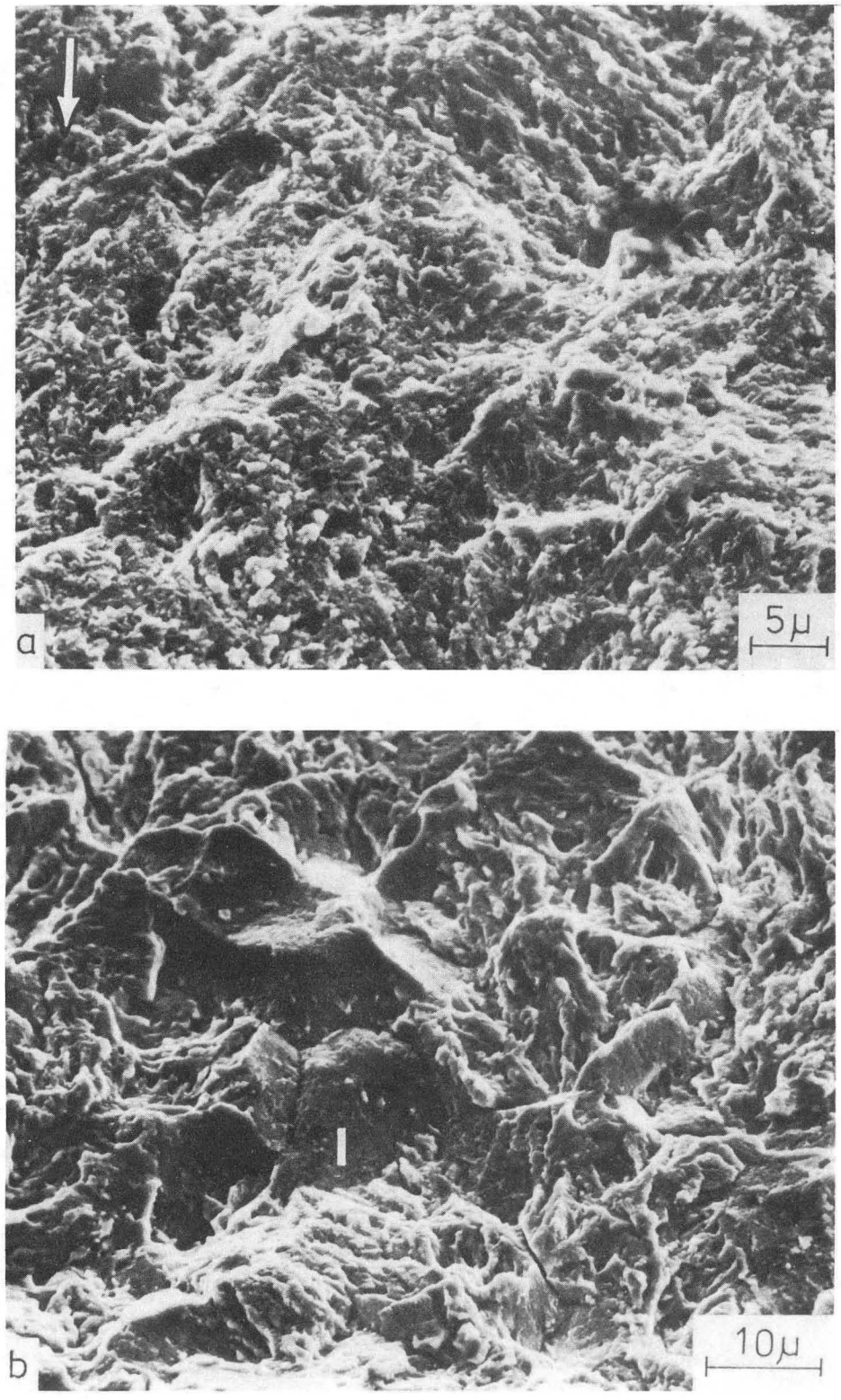

XBB 764-3784

Fig. 7. Morphology of fatigue fracture at near-threshold crack growth rates at $\Delta K = 9.5$ MPa$\sqrt{m}$ (R=0.05) in 300-M steel showing a) ductile transgranular mechanism in unembrittled material, and b) segments of intergranular fracture (I) in temper embrittled material. (Arrow indicates general direction of crack propagation).

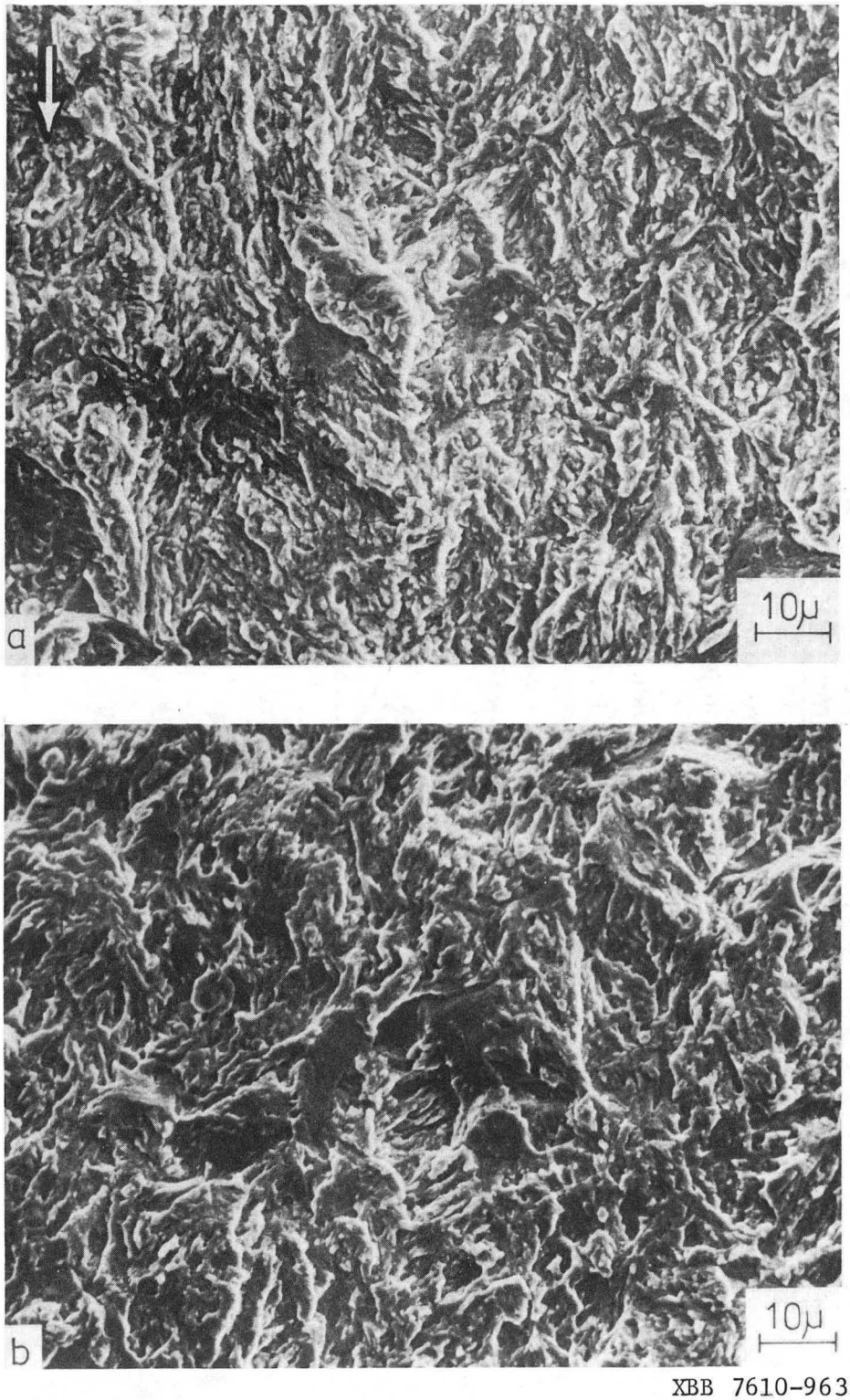

XBB 7610-9633

Fig. 8. Morphology of fatigue fracture at ΔK = 15 MPa$\sqrt{m}$ (R=0.05) in 300-M steel in a) unembrittled and b) temper embrittled material. (Arrow indicates general direction of crack propagation.)

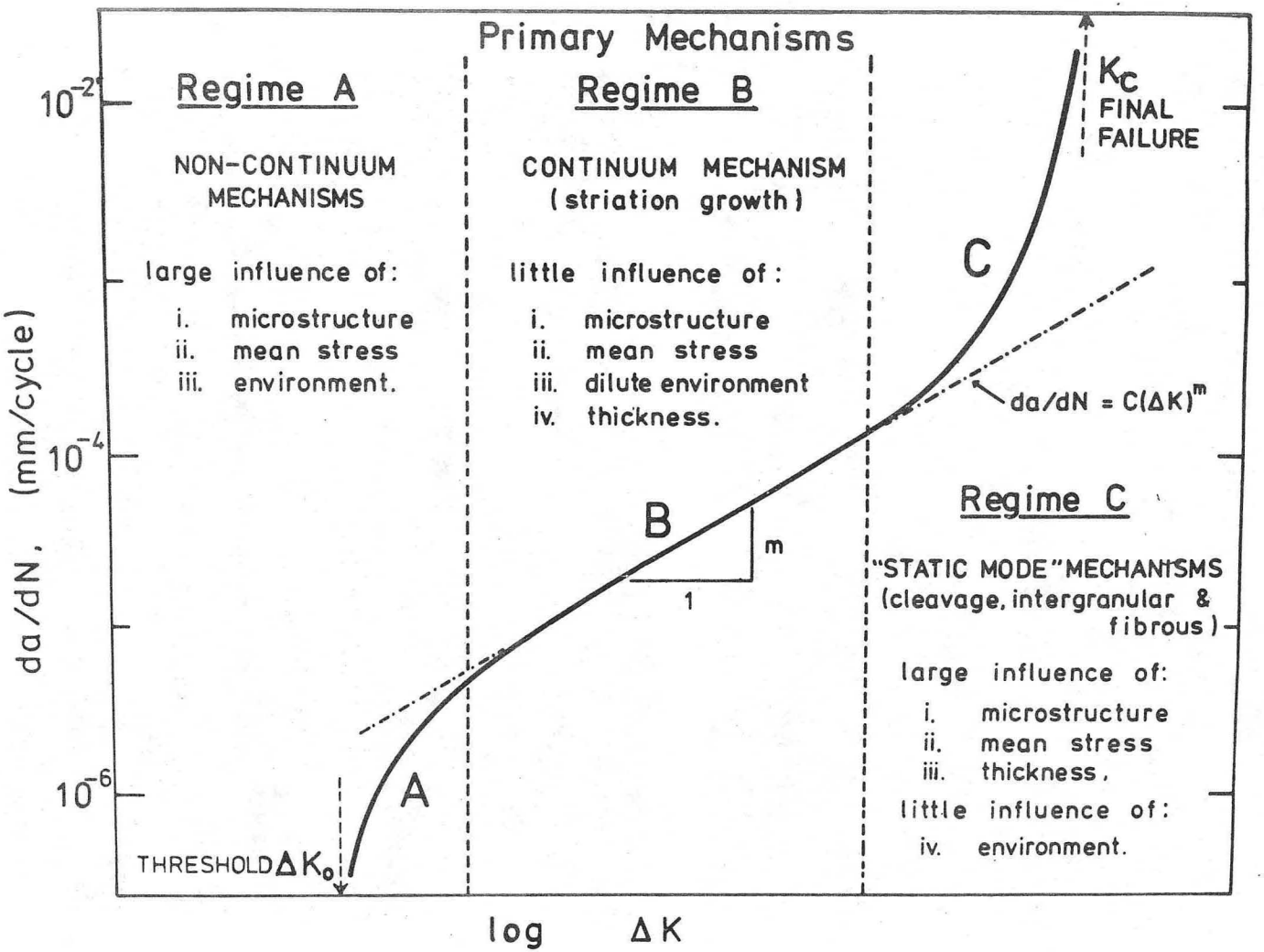

XBL 754-1019

Fig. 9. Schematic diagram showing the primary fracture mechanisms and associated fatigue behavior consistant with the sigmoidal variation of fatigue crack propagation rate (da/dN) with alternating stress intensity (ΔK). ΔK_o is the threshold stress intensity for crack growth, K_c the stress intensity at final failure.

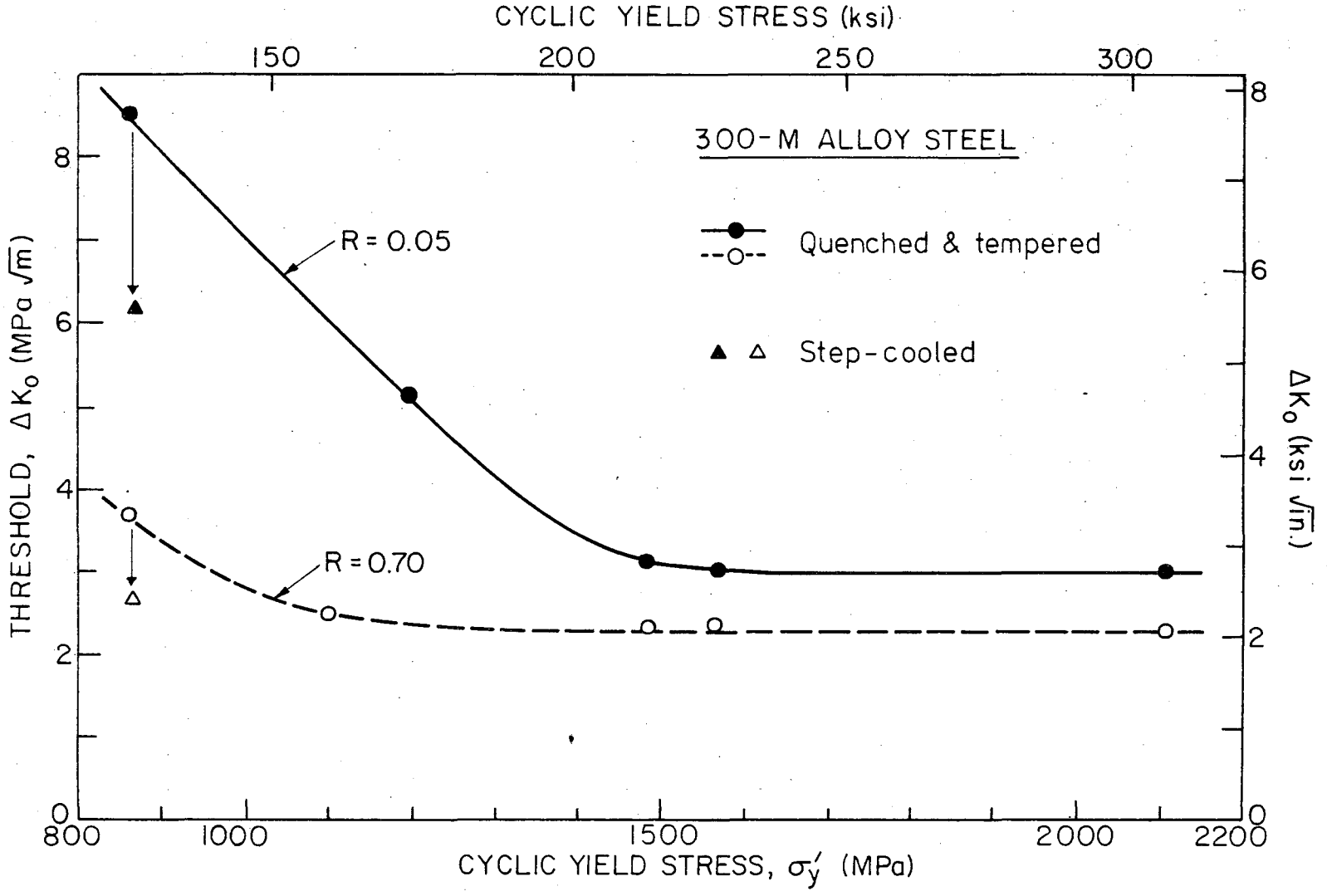

XBL 768-7289C

Fig. 10. Influence of cyclic strength on the threshold for fatigue crack growth (ΔK_o), at R=0.05 and 0.70, for quenched and tempered 300-M steel, showing additional effect of temper embrittlement, induced by step-cooling.

TECHNICAL INFORMATION DIVISION
LAWRENCE BERKELEY LABORATORY
UNIVERSITY OF CALIFORNIA
BERKELEY, CALIFORNIA 94720